Spectra of particles from laser-induced vacuum decay

Lance Labun and Johann Rafelski

Spectra of Particles from Laser-Induced Vacuum Decay

Lance Labun and Johann Rafelski

Department of Physics, University of Arizona, Tucson, Arizona, 85721 USA

The spectrum of electrons and positrons originating from vacuum decay occurring in the collision of two non-collinear laser pulses is obtained. It displays high energy, highly-collimated particle bunches traveling in a direction separate from the laser beams. This result provides an unmistakable signature of the vacuum decay phenomenon and could suggest a new avenue for development of high energy electron and/or positron beams.

I. INTRODUCTION

Quantum Electrodynamics implies that when the potential difference in an electromagnetic field exceeds $2mc^2$ in constant [1, 2] and non-constant fields [3], the field-filled domain decays by particle emission. Many other effects of the quantum-induced nonlinearity have been studied over the years, including photon-splitting [4, 5], the energy-momentum trace [6–8] and vacuum birefringence [9, 10]. None of these effects has yet been experimentally observed.

A plane electromagnetic wave of arbitrary intensity and wavelength composition is absolutely stable against pair materialization decay [2], since there is no reference frame in which massive decay products can appear. Colliding laser pulses can form a field configuration that does have a preferred reference frame: the frame in which the local field momentum density (the Poynting vector) vanishes defines the local rest frame in which decay products can materialize. The field energy present in this frame is the amount available for materialization [11].

In fact, any electromagnetic field configuration having an identifiable reference frame can decay, and will decay for any positive value of the invariant

$$d^2 = \sqrt{\mathcal{S}^2 + \mathcal{P}^2} - \mathcal{S} > 0, \qquad (1)$$

$$\mathcal{S} = \frac{1}{2}(\vec{B}^2 - \vec{E}^2), \quad \mathcal{P} = \vec{E} \cdot \vec{B} \qquad (2)$$

A previously in-depth studied example is pair production by a super-critical Coulomb potential near a $Z > 173$ nucleus [12]. There, the bare charge of the at-rest nucleus is screened by the charged vacuum state [13] localized around the nucleus, and a positron escapes. If and when the super-critical potential dissociates, the localized electron charge from the charged vacuum state could also be freed, completing the pair formation process.

Many studies have addressed pair creation in intense laser pulses colliding head-on [14–27] (since this offers the highest particle yield) or traveling parallel [28–32] (since chirped laser pulses consist of many focused frequency components). In this work we show how one obtains spectra of produced particles in laboratory by identifying the frame of reference in which production occurs. We evaluate for the case of non-collinear colliding lasers, a field configuration whose local rest frame moves at high rapidity with respect to the laboratory. The advantages of this geometry are that 1) nearly monochromatic bunches of high energy particles are produced, and 2) the bunches are boosted in the direction of the Poynting vector of the combined laser pulses and thus away from each individual laser pulse. These characteristics constitute a signal that the pairs originate in vacuum decay, which from standpoint of discovery potential outweighs the reduction in particle yield as compared to head-on collisions. Mirroring the practice in elementary particle physics, the decay rates and products are studied in this work in terms of Lorentz invariants, keeping separate the particle production process from the reference frame determination.

II. RAPIDITY OF MOVING REST FRAME

In the laboratory frame characterized by a 4-velocity $u^K = (1, \vec{0})$ the 4-momentum density is $p^K = T^{KJ}u_J$ using the energy-momentum tensor T^{KJ}. The energy density p^0 and the Poynting momentum density p^i of an electromagnetic field configuration are

$$p^0 = \varepsilon \frac{\vec{E}^2 + \vec{B}^2}{2} + \frac{T_K^K}{4}, \qquad p^i = \varepsilon(\vec{E} \times \vec{B})^i =: \vec{S}. \quad (3)$$

The dielectric shift $\varepsilon - 1$ and the energy-momentum trace T_K^K vanish in classical electromagnetism and acquire non-zero field dependent values in QED due to fluctuations in the vacuum [8].

The (square) invariant mass density $\mu^2 = u_J T_K^J T^{KJ'} u_{J'}$ can be studied in any frame of reference, in particular in the lab frame or in the frame having $\vec{S} = 0$ where energy density is rest mass density. We proceed to evaluate mass density in the lab frame. Using the explicit expression for the electromagnetic energy-momentum tensor we obtain [8, 11]

$$\mu^2 := p_K p^K = \varepsilon^2 (\mathcal{S}^2 + \mathcal{P}^2) + (T_K^K/4)^2. \qquad (4)$$

For general field configurations, μ is a function of space and time and determines the instantaneous, local rapidity y_S of the moving rest frame

$$\cosh^2 y_S = \frac{\mu^2 + \varepsilon^2(\vec{E} \times \vec{B})^2}{\mu^2} = 1 + \frac{\vec{S}^2}{\mu^2} = \frac{(p^0)^2}{\mu^2} \qquad (5)$$

which exhibits the dependence on the geometric relation between the electric and magnetic field vectors. As for particles, large electromagnetic momentum density $|\vec{S}| > \mu$ in a given frame corresponds to high rapidity. Note that the choice $u^K = (\cosh y_S, 0, 0, \sinh y_S)$ produces the corresponding result for mass density working in the local CM frame.

An isolated electric field is at rest in the laboratory. In the presence of any magnetic field along with the electric field, the total field configuration acquires momentum dependent on the angle between the electric and magnetic field vectors, seen in the non-zero Poynting vector Eq. (3). If the magnetic field is orthogonal to the electric field ($\mathcal{P} = 0$), a frame exists where one of $\vec{E}, \vec{B}$ vanishes and is the rest frame. Otherwise, when $\mathcal{P} \neq 0$ the frame where $\vec{E}, \vec{B}$ are parallel is the rest frame.

Consider the example of a linearly polarized plane wave entering a domain of quasi-constant magnetic field. The largest quasi-static magnetic fields in laboratory are small in comparison to the fields available in pulsed laser systems, and the ratio of the external field to the laser field strength

$$\frac{eB_{\text{ext}}}{a_0 \omega m} < 10^{-4}, \quad a_0 := \frac{e|A^K|}{m} = \frac{e|\vec{E}_{\text{laser}}|}{\omega m} \qquad (6)$$

where a_0 is the dimensionless laser amplitude and ω is the laser frequency. The resulting superposition of fields has a small mass density and a large rapidity. The same choices for field geometry that provide a large y_S reduce the magnitude of μ due to the finite total energy density being apportioned between rest mass density and momentum density by $\cosh y_S$.

For a present day high-intensity laser with $\omega \simeq 1$ eV and $a_0 = 100$ and an external magnetic field of 1T aligned with the laser polarization, the resultant mass density $\mu(x,t)$ and rapidity $y(x,t)$ at each position and time are

$$\mu(x,t) \lesssim 5\,10^8 \frac{\text{MeV}}{\text{nm}^3}, \quad y(x,t) \gtrsim 14. \qquad (7)$$

This μ is 14 orders of magnitude smaller than the scale set by the electron $0.511\,\text{MeV}/\lambda_e{}^3 = (e\vec{E}_c)^2$ where $|\vec{E}_c| = m^2 c^3/e\hbar = 1.3 \times 10^{18} \text{V/m} = 4.4 \times 10^9\,c\text{T}$, and too small to generate a significant number of electron-positron pairs.

III. MATERIALIZATION OF ELECTRON-POSITRON PAIRS

Decay of the unstable field into an electron-positron pair is treated as a semi-classical tunneling process [33], which shows the momentum distribution to be dominantly Gaussian. Due to the adiabatic $\omega \ll m_e$ turn-on of the field, particles are created at threshold with zero momentum $p_\parallel = 0$ in the direction of the electric field in the field's moving rest frame, and the energy E_p of the outgoing particle depends only on the momentum $\vec{p}_\perp^2$

perpendicular to electric field. The tunneling probability

$$\Gamma \propto e^{-\pi E_p^2/ed}, \qquad E_p^2 = \vec{p}_\perp^2 + m^2. \qquad (8)$$

and other pertinent quantities depend on the field invariants $d^2 = \sqrt{\mathcal{S}^2 + \mathcal{P}^2} - \mathcal{S} \to |\vec{E}|^2$ and $b^2 = \sqrt{\mathcal{S}^2 + \mathcal{P}^2} + \mathcal{S} \to |\vec{B}|^2$ which reduce to the corresponding electric and magnetic magnitudes in the moving rest frame of the field. Deriving the spectrum requires knowing the orientation of the field: $\vec{p}_\perp$ above is the electron (positron) momentum transverse to the direction of the electric field vector present in the moving rest frame of the decaying field. Note that transforming to the laboratory frame preserves the Gaussian shape.

The total number of expected pairs $\langle N \rangle$ is obtained by integrating Eq. (8) over transverse momenta and multiplying by total volume and time over which the unstable field configuration ($E^2 - B^2 > 0$) exists [34, 35]

$$\frac{1}{VT}\langle N \rangle = \frac{e^2 bd}{8\pi^2} \coth\left(\frac{\pi b}{d}\right) e^{-\frac{\pi m^2}{ed}} \xrightarrow[b \to 0]{} \frac{(ed)^2}{8\pi^3} e^{-\frac{\pi m^2}{ed}}, \quad (9)$$

The rate at which field energy is converted into material particles is computed by weighting the momentum integral with the energy of the particle, giving [11]

$$\frac{d\langle u_m \rangle}{dt} \simeq \frac{\alpha m}{\pi^2} d^2 e^{-\pi m^2/ed}. \qquad (10)$$

The characteristic time for conversion of field energy into particles usually far exceeds the laboratory duration of the field. For $d \gtrsim 0.1|\vec{E}_c|$ however, pair creation becomes copious and the lifetime approaches the time scale of the laser pulses composing the field. Consequently, the fraction of field energy converted into particles becomes large and detailed treatment of backreaction is necessary [36, 37].

IV. COLLIDING LASER PULSES AND PARTICLE SPECTRA

As the strongest available electromagnetic fields are today created with pulsed lasers, colliding pulses offers the best means to maximize d and create unstable field configurations. Judicious choice of collision geometry creates a region where both the rapidity y and the electric invariant d are large. Figure 1 illustrates two linearly-polarized laser waves $\vec{k}_{\text{w}}, \vec{k}_{\text{s}}$ (superscript-w for 'weak' and -s for 'strong'), converging at an angle θ with electric field vectors $\vec{E}_{\text{s}}, \vec{E}_{\text{w}}$ aligned in the $x_\parallel$-direction. The wave vectors $k_{\text{w}}, k_{\text{s}}$ define the $x_{\perp,1}$-$x_{\perp,2}$ collision plane, in which the collision angle θ varies between exactly collinear laser pulses $\theta = 0$ and a head-on collision $\theta = \pi$.

The Poynting momentum of the total field $\vec{S}_{\text{tot}}$ is determined by the net magnetic field: the vector sum of the lasers' magnetic fields deflects $\vec{S}_{\text{tot}}$ away from the beam line of the 'strong' (s) laser by an angle δ given by

$$\tan \delta = \frac{r \sin \theta}{1 + r \cos \theta}; \quad r = \frac{a_0^{\text{w}} \omega^{\text{w}}}{a_0^{\text{s}} \omega^{\text{s}}} \leq 1 \qquad (11)$$
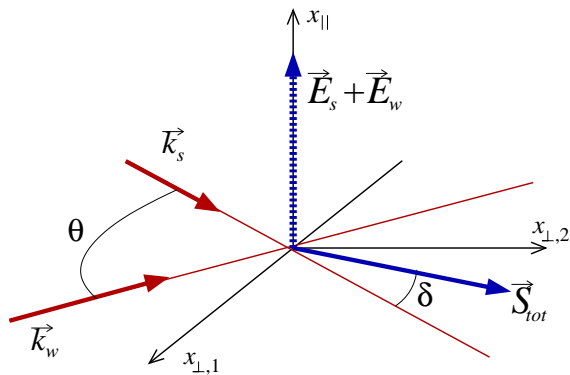
FIG. 1: Schematic of two converging linearly-polarized laser waves, $\vec{k}_s, \vec{k}_w$, with $\vec{E}_s, \vec{E}_w$ the corresponding electric field vectors. $\vec{S}_{tot}$ is the Poynting vector of the resultant field, deflected an angle δ by the second laser pulse. (Color online.)

$\vec{S}_{\text{tot}}$ is in the plane normal to the electric field (the collision plane) also when considered in the moving rest frame of the field. $\vec{p}_\perp$ of produced particles is in this collision plane. Upon boosting by rapidity y_S to the lab frame, the Gaussian distribution, which is uniform in $\vec{p}_\perp$ in the moving rest frame, is shifted in one of the two transverse components, remains centered around zero in the other transverse momentum component and remains negligible in direction parallel to the electrical field.

For a qualitative model, we take square-wave-localized pulses. Setting the waves to be in phase, the oscillation within each individual pulse results in a checker-board of stable ($E^2 - B^2 < 0$) and unstable ($E^2 - B^2 > 0$) subdomains in the volume where the pulses overlap. The stable subdomains do not contribute to the particle output. Within the unstable domains the individual sinusoidal variations of the laser fields produce a variation in the direction and magnitude of $\vec{S}_{\text{tot}}$. However, most particles are created near the peak of the sinusoid where variation of $\vec{S}_{\text{tot}}$ is slow. Space and time dependence of the fields affects particle yields by a factor of order unity and spectra by small changes to distribution widths. In the following, we evaluate using the peak field magnitudes and geometry.

In unstable subdomains, the magnetic field is reduced by $\cos\theta$ in magnitude compared to the net electric field and remains orthogonal to it. As a result,

$$b^2 = 0, \quad (ed)^2 = 2r(1 - \cos\theta)(a_0^s \omega^s m)^2. \quad (12)$$

We consider three cases: equal intensity $r = 1$, and 'weak deflections' $r = 0.1, = 0.01$. The rapidity y is shown on the left axis in Fig. 2 with corresponding three lines merging at small θ at large y (from top to bottom: small r to $r = 1$). For the collision of equal intensity pulses $r = 1$ the rapidity goes to zero approximately linearly as $\theta \to \pi$, reflecting that standing waves created by counter-propagating square laser pulses are at rest in the laboratory. In the asymmetric $r < 1$ cases, the weak laser field serves similar to the quasi-constant external field exam-

ple above, giving the strong laser pulse a mass density and the ability to decay at relatively high rapidity y_S.

To create pairs with initially high rapidity in the lab, we focus on $\theta < \pi/2$. The number of pairs obtained would be maximized for the head-on collision $\theta = \pi$, but in this case the pair-producing field is at rest in the lab and the pairs appear with zero net momentum. Decreasing θ results in higher rapidities, but in order to maintain the same yield in particles, intensity of the field in the collision domain must be increased, whether by increasing the intensity of the strong pulse a_0^s or the ratio r. In the limit $\theta \to 0$, the mass density (and hence the potential for pair production) vanishes because the converging laser pulses have degenerated into collinearly propagating waves.

As for the above example of a laser field incident on an external magnetic field, the trade-off between yield of produced pairs and rapidity of the moving rest frame is a consequence of the finite total energy density of the laser pulses. This trade-off is visible in the θ dependence of the invariant mass density, which derives from nonvanishing d^2 in the region of superposition,

$$\mu^2 = 2\varepsilon^2 r^2 (1 - \cos\theta)^2 + (T_K^K/4)^2. \quad (13)$$

The rapidity of the moving rest frame of the field is

$$\sinh^2 y_S = \frac{\left[\left(\frac{1}{2}(r^{-1} + r)\csc^2(\theta/2) + \cot^2(\theta/2)\right]^2 - 1}{1 + \left(T_K^K/4\varepsilon d^2\right)^2} \quad (14)$$

For the strong fields necessary to induce significant pair creation, $T_K^K/4$ is a noticeable correction, comparable in magnitude to focusing corrections. In generating Figure 2, we have used non-perturbatively computed values of ε and T_K^K [8]. For $d \lesssim 0.1|\vec{E}_c|$ their series expansions, given in [8], can be used to good accuracy.

In the laboratory frame, the vacuum-derived pairs have a boosted mean momentum $\langle p_{\parallel S} \rangle = \sqrt{m^2 + p_T^2}\sinh(y - y_S)$ in the direction of $\vec{S}_{\text{tot}}$, thus defining direction of the bunch. In the plane normal to $\vec{S}_{\text{tot}}$, the produced particles have a momentum distribution concentrated in the direction that is perpendicular also to the net electric field vector. In this direction, the p_T momentum distribution is Gaussian with mean zero, unaffected by the Lorentz transformation along $\vec{S}_{\text{tot}}$. With high rapidity and low transverse momenta, the vacuum-decay products form a pancaked, tightly collimated bunch with low transverse emittance. Distributions in rapidity $y_p = y - y_S$ and transverse momentum p_T are shown in Fig. 3 for four selected collision angles $\theta = 8\pi/16, 6\pi/16, 5\pi/16, 4\pi/16$. To the left, we see the transverse momentum distribution. To right, we see normalized distribution in y_p, integrated over p_T.

The spatial size of the produced particle bunch is determined by the size of collision volume and hence for lasers focused near to the diffraction limit is $\sim \lambda^3 = (1\,\mu m)^3$. Note that charge separation due to the definite orientation of the electric field implies that the positrons appear separated from the electrons by about the width
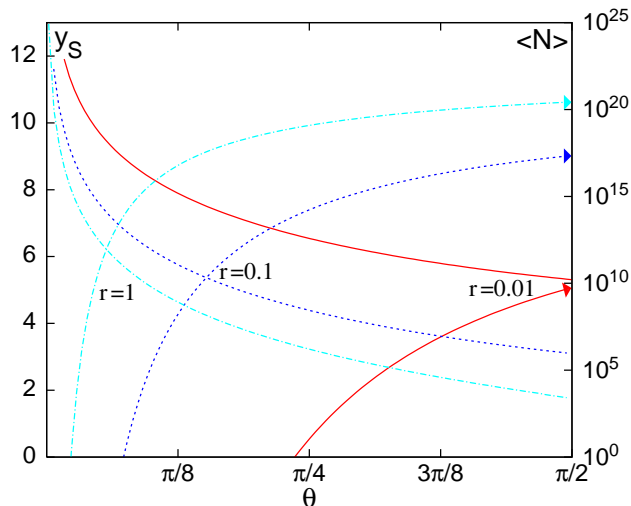

FIG. 2: The rapidity y_S of the moving rest frame (left scale) and expected number of pairs (right scale, lines with arrows) for $r = 1$, 0.1, 0.01 at fixed $a_0^s \omega^s/m = 1$. (Color online.)
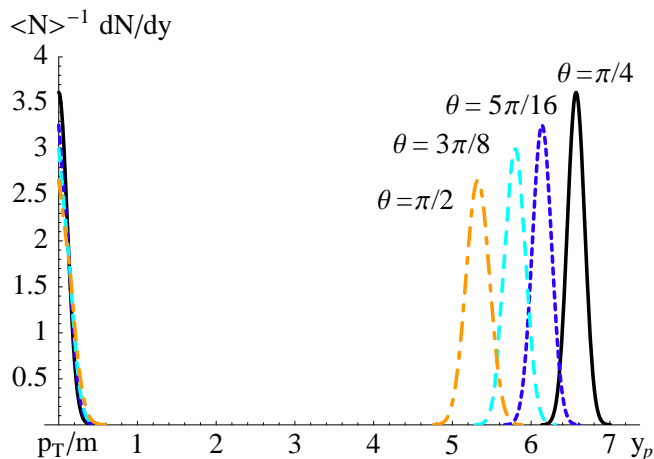

FIG. 3: The normalized distributions in rapidity and transverse momentum for $a_0^s \omega^s/m = 1$, $r = 10^{-2}$ and $\theta = \pi/2$, $3\pi/8$, $5\pi/16$, and $\pi/4$. To the left p_T/m spectra and to the right the rapidity spectra. See text for specific meaning of p_T. (Color online.)

of the pulse. As $\langle N \rangle$ is an extensive quantity, we com-

pute reference values for a collision volume × duration of $(5\lambda)^3 \times 25\lambda/c$. Fig. 2 exhibits the trade-off between $y, \langle N \rangle$ (right scale, lines with arrows), which arises from the trade-off between y_S, μ noted above.

V. CONCLUSIONS

The field rest frame is general to classical electromagnetism of Maxwell's equations and applies to most superpositions of laser pulses. We showed how the invariant mass density and the rapidity of the moving rest frame are controlled. For the example of two colliding high-intensity square laser pulses, we showed how to create collimated high energy electron-positron bunches that are directed away from both laser beam lines and may be directed independently after creation. The resulting bunches are planar in the plane normal to the electric field and Gaussian in momentum.

We have discussed how the total energy of the unstable field configuration can be smoothly allotted between the energy per particle and total number of particles in the bunch. In the present model, the particle number in the resultant bunch depends most on the absolute magnitude of the fields attained in the collision volume. Techniques such as optimizing pulse shape [19] and frequency structure [24, 26] can be applied to enhance the yield.

Particles are produced in their rest frame at a very low energy, and the high laboratory energy is achieved by superposing nearly collinear, pulsed electromagnetic fields so as to have the rest frame moving at high rapidity relative to the lab. No acceleration process is needed to bring the charged particles to high energy. In our proposed beam geometry the laser fields may be made very strong without endangering the stability of the experiment or its apparatus by near-critical laser pulses. The vacuum decay products in laser pulse collisions are readily distinguishable from particle-creation backgrounds such as cascades [38] and perturbative processes thus enhancing discovery potential. The concept we have described may permit future development of a source of particles with ultra-high energy.

[1] W. Heisenberg and H. Euler, Z. Phys. **98**, 714 (1936).
[2] J. S. Schwinger, Phys. Rev. **82**, 664 (1951).
[3] F. Sauter, Z. Phys. **73**, 547 (1932).
[4] S. L. Adler, J. N. Bahcall, C. G. Callan, M. N. Rosenbluth, Phys. Rev. Lett. **25**, 1061-1065 (1970); S. L. Adler, Annals Phys. **67**, 599-647 (1971); S. L. Adler, C. Schubert, Phys. Rev. Lett. **77**, 1695-1698 (1996).
[5] Z. Bialynicka-Birula and I. Bialynicki-Birula, Phys. Rev. D **2**, 2341 (1970).
[6] S. L. Adler, J. C. Collins, A. Duncan, Phys. Rev. **D15**, 1712 (1977).
[7] W. Dittrich, M. Sieber, J. Phys. **A21**, L711-L714 (1988).
[8] L. Labun and J. Rafelski, Phys. Rev. D **81**, 065026 (2010).
[9] Z. Bialynicka-Birula, Physica D **2**, 513 (1981).
[10] S. L. Adler, J. Phys. A **40**, F143 (2007).
[11] L. Labun and J. Rafelski, Phys. Rev. D **79**, 057901 (2009).
[12] W. Greiner, B. Muller and J. Rafelski, *Quantum Electrodynamics Of Strong Fields* (Springer, Berlin, 1985).

[13] J. Rafelski, B. Muller and W. Greiner, Nucl. Phys. B **68**, 585 (1974).

[14] E. Brezin and C. Itzykson, Phys. Rev. D **2**, 1191 (1970).

[15] N. B. Narozhny and A. I. Nikishov, Zh. Eksp. Teor. Fiz. **65**, 862 (1973).

[16] R. Alkofer, M. B. Hecht, C. D. Roberts, S. M. Schmidt and D. V. Vinnik, Phys. Rev. Lett. **87**, 193902 (2001).

[17] H. M. Fried, Y. Gabellini, B. H. J. McKellar and J. Avan, Phys. Rev. D **63**, 125001 (2001).

[18] H. K. Avetissian, A. K. Avetissian, G. F. Mkrtchian, K. V. Sedrakian, Phys. Rev. E. **66** 016502 (2002).

[19] A. Di Piazza, Phys. Rev. D **70**, 053013 (2004).

[20] D. B. Blaschke, A. V. Prozorkevich, C. D. Roberts, S. M. Schmidt and S. A. Smolyansky, Phys. Rev. Lett. **96**, 140402 (2006).

[21] A. R. Bell and J. G. Kirk, Phys. Rev. Lett. **101**, 200403 (2008).

[22] M. Ruf, G. R. Mocken, C. Muller, K. Z. Hatsagortsyan and C. H. Keitel, Phys. Rev. Lett. **102**, 080402 (2009).

[23] J. G. Kirk, A. R. Bell and I. Arka, Plasma Physics and Controlled Fusion **51**, 085008 (2009).

[24] G. V. Dunne, H. Gies, R. Schutzhold, Phys. Rev. **D80**, 111301 (2009).

[25] S. S. Bulanov, V. D. Mur, N. B. Narozhny, J. Nees and V. S. Popov, Phys. Rev. Lett. **104**, 220404 (2010).

[26] C. K. Dumlu and G. V. Dunne, Phys. Rev. Lett. **104**, 250402 (2010)

[27] S. S. Bulanov, T. Z. Esirkepov, A. G. R. Thomas, J. K. Koga and S. V. Bulanov, Phys. Rev. Lett. **105**, 220407 (2010).

[28] A. Ringwald, Phys. Lett. B **510**, 107 (2001).

[29] N. B., Narozhny, *et al.*, Phys. Lett. A **330**, 1 (2004).

[30] R. Schutzhold, H. Gies and G. Dunne, Phys. Rev. Lett. **101**, 130404 (2008).

[31] B. King, A. Di Piazza, and C. H. Keitel, Phys. Rev. **A82**, 032114 (2010).

[32] C. K. Dumlu, Phys. Rev. D **82**, 045007 (2010).

[33] A. Casher, H. Neuberger and S. Nussinov, Phys. Rev. D **20**, 179 (1979).

[34] A. I. Nikishov, Nucl. Phys. B **21**, 346 (1970).

[35] T. D. Cohen and D. A. McGady, Phys. Rev. D **78**, 036008 (2008).

[36] F. Cooper, J. M. Eisenberg, Y. Kluger, E. Mottola and B. Svetitsky, Phys. Rev. D **48**, 190 (1993).

[37] B. Mihaila, F. Cooper and J. F. Dawson, Phys. Rev. D **80**, 014010 (2009).

[38] A. M. Fedotov, N. B. Narozhny, G. Mourou and G. Korn, Phys. Rev. Lett. **105**, 080402 (2010).